J Mater Sci (2009) 44:4013–4019
DOI 10.1007/s10853-009-3552-2

Microstructural characterisation of syntactic foams

Imre N. Orbulov · Janos Dobranszky · Arpad Nemeth

Received: 4 February 2009 / Accepted: 5 May 2009 / Published online: 22 May 2009

Abstract Three types of hollow microspheres with different average diameters (100–150 μm) and two aluminium alloys as matrix material were used to produce metal matrix syntactic foams (MMSFs) by pressure infiltration. The phases, which formed at matrix-filler interface, were investigated by X-ray diffraction (XRD) and energy dispersive spectrometry (EDS). The investigation showed that in syntactic foams, with the Al99.5 matrix, an exchange reaction took place between the matrix and the amorphous components of ceramic hollow microspheres. The reaction resulted in significant formation of alumina and Si precipitates. Because of this diffusion reaction, the hollow microspheres' walls were degraded. In the case of the AlSi12 matrix the reaction was suppressed by the considerable Si content of the matrix. Therefore, the wall of the hollow microspheres remained unharmed and no real interface layer was found.

Introduction

Particle-reinforced composites have a special class called 'syntactic' foams. The first publications on this material were presented in the late 60s. Kallas and Chatten [1] were among the first researchers who investigated these materials. The first syntactic foams had polymer matrix and they have been widely studied by many authors [2–5]. Other non-metallic matrix materials are used—for example starch—in civil engineering and building technology [6]. Nowadays, metal matrices are used in many cases. In metal matrix syntactic foams (MMSFs) the porosity is originated from low density ceramic hollow microspheres, which are compositions of various oxides, mainly SiO_2, Al_2O_3, K_2O, Fe_2O_3 and MgO. Due to their low density the MMSFs have perspective applications in covers, castings, furniture and engine blocks in the automotive and electromechanical industry sectors. Other advantages of metal matrix syntactic foams are high specific compression strength and thermal stability. Therefore, they are also used as energy absorbers, sound absorbers or as material for the hulls in submarine applications and aeronautics.

The production and properties of metal matrix syntactic foams have been widely studied. They are usually made by pressure infiltration or by a blending method. Ramachandra and Radhakrishna [7, 8] described the blending method in detail and investigated the wear mechanism and hardness of the foams produced. This method is relatively easy to implement, but it is hard to be applied when a higher volume fraction of hollow microspheres is required due to rheological and other (fracture of the hollow microspheres) effects. Therefore, pressure infiltration was also investigated. This method is the easiest to produce particle reinforced metal matrix composites with high reinforcement volume fraction. For example, Rohatgi et al. [9, 10] applied pressure infiltration to produce syntactic foams and investigated their compressive properties. In other investigations syntactic foams were also produced by pressure infiltration and their failure mechanism was studied during upsetting in

I. N. Orbulov (✉) · A. Nemeth
Department of Materials Science and Engineering, Budapest University of Technology and Economics, Goldmann Gy. tér 3, Budapest 1111, Hungary
e-mail: orbulov@gmail.com

J. Dobranszky
Research Group for Metals Technology of the Hungarian Academy of Sciences, Goldmann Gy. tér 3, Budapest 1111, Hungary

annealed and heat-treated conditions [11]. The effect of SiCp addition on age-hardening was also investigated. The authors found the addition of SiCp influences the optimal ageing time significantly [12]. On the other hand, the compressive characteristics of the syntactic foams are extremely important, because compression is the main load type in the case of their potential applications. Therefore, the compression behaviours have been widely studied [13–16]. Palmer et al. [17] applied different aluminium matrices and investigated their mechanical properties by upsetting, tensile and bending tests. For successful pressure infiltration a threshold pressure must be ensured, which can be estimated by using theoretical and experimental methods. Bárczy and Kaptay [18] developed a theoretical method by considering the wetting angle, surface tension and based on the equilibrium of gravitational, capillary and outer forces. It would be somewhat simpler to define a hydraulic radius, depending on the shape and volume fraction of the hollow microspheres and apply the Young-Laplace equation to evaluate threshold pressure [19]. A very similar method can be done by determining the effective distance between the hollow microspheres [10].

The matrix of the metallic syntactic foams is usually aluminium alloy because of its low density, relatively low melting point and good castability. Between the hollow microspheres and the matrix, an interface layer can be formed. This layer has a very important role in mechanical properties, because it ensures the load transfer between the hollow microspheres and the matrix. In a previous study, load partitioning was investigated by using neutron and synchrotron X-ray diffraction (XRD) analysis [20]. The interface layers, formed during production, have at least the same importance in syntactic foams as the constituents themselves. Therefore, the investigation of interface layers should be one of the most important tasks in characterisation. From the results of XRD and energy dispersive spectrometry (EDS) investigations on syntactic foams and their constituents, one can deduce conclusions about the interface layers, and therefore about the properties of the foam itself. The aim of this study is to investigate and characterise the interface layers formed in aluminium matrix syntactic foams.

Experimental

Metal matrix syntactic foams were produced by pressure infiltration. The furnace system used for this work can provide temperatures from 20 to 1200 °C at pressures from rough vacuum to 10 MPa. Lightweight Al99.5 and AlSi12 alloys were applied as matrix materials. The fillers were E-sphere type hollow microspheres supplied by Enviro-spheres Pty. Ltd. [21]. Three types of E-spheres were used as fillers, SL150, SLG and SL300, respectively. We used a buoyant method to eliminate broken hollow microspheres from a batch. Table 1 below, shows the constituent phases and average diameters of the hollow spheres (the values were supplied by the manufacturer, except the size range published in [6]).

In summary, six types of MMSF blocks were produced. Their dimensions were 36 × 55 × 170 mm^3. The hollow microsphere content was maintained at 64 vol.%. The parameters of the pressure infiltration are shown in Table 2 below. The pressure was ensured by using argon gas and it was maintained for 30 s. After the infiltration the blocks were cooled by water. The specimens were investigated in 'as-produced' state and they were named after their constituents. For example, the name AlSi12-SLG means the specimen has AlSi12 aluminium alloy matrix and approx. 64 vol% SLG type hollow microspheres.

XRD and EDS analyses were carried out in order to obtain information in relation to the interface between the reinforcement and matrix material. All XRD analyses were performed on powdered specimens at the Chemical

Table 2 The temperature and pressure data of the infiltration processes

Specimen	Temperature of infiltration (°C)	Infiltration pressure (kPa)
Al-SL150	715	442
Al-SLG	720	441
Al-SL300	690	426
AlSi-SL150	630	355
AlSi-SLG	630	342
AlSi-SL300	600	346

Table 1 Morphological properties and phase constitution of the applied hollow ceramic spheres (provided by the manufacturer, except the size range published in [6])

Type	Average diameter (μm)	Size range (95%) (μm)	Specific surface (μm^{-1})	Al_2O_3	Amorphous SiO_2	Mullite	Quartz	Other
SL150	100	56–183	0.060	30–35%	45–50%	19%	1%	Bal.
SLG	130	85–233	0.046					
SL300	150	101–332	0.040					

Research Centre of the Hungarian Academy of Sciences. Here, the Philips X–Pert type diffractometer was used with 35 mA cathode heating current, copper anode ($\lambda =$ 0.154186 nm) with 40 kV voltage. The rotating speed of the goniometer was 0.04 °/s. Small, but representative parts ($\sim$1 cm^3) of the MMSFs were dry powdered in alumina mortar.

The EDS investigations were performed by using a Phillips XL-30 type scanning electron microscope with EDAX Genesis analyser. EDS line analysis was performed to characterise the elemental distribution at the interfaces of MMSFs, where the hollow microspheres were in contact with the matrix. All EDS line analysis of the elemental distribution was performed on polished surfaces, where the excitation voltage was 15 kV. The measurement started from the matrix materials and crossed the wall of the hollow sphere. Thirty points were measured along each line.

Results and discussion

First of all we determined the density and porosity of the MMSFs (Table 3), because excessive entrapped porosity or microsphere fracture can be estimated from these results. The densities were measured according to Archimedes' law. The added porosity can be sorted into two groups: planned porosity, which was ensured by the microspheres (P_{mb}) and unintended porosity (P_{up}), which was caused by insufficient infiltration between the small microspheres. The planned (or microsphere) porosity can be calculated as follows.

$$P_{mb} = V_{mb}\left(\frac{r_i}{r_o}\right)^3 \quad (1)$$

where V_{mb} is the volume fraction of the microspheres in the MMSF; maintained at 64 vol.% in all cases. The radii r_i and r_o are the average inner and outer radii of the microspheres, respectively. These radii were calculated from the average diameters of the microspheres, density of the pure microspheres, and the density of the wall of the microspheres. The unintended porosity can be calculated as:

$$P_{up} = \frac{\rho_t - \rho_m}{\rho_t} \quad (2)$$

where ρ_t and ρ_m are the theoretical and measured densities of the syntactic foams, respectively. The theoretical density was calculated by the rule of mixture from the density of the microspheres and the matrix. The ideal syntactic foam has no unintended porosity. The total porosity (P_{tp}) is equal with the sum of planned and unintended porosity.

$$P_{tp} = V_{mb}\left(\frac{r_i}{r_o}\right)^3 + \frac{\rho_t - \rho_m}{\rho_t} \quad (3)$$

In general, the unintended porosity is rather small so the infiltration was almost perfect. However, in the case of the Al99.5 matrix the unintended porosity has a negative value, which means that in some cases the infiltration of microspheres occurred. Therefore, the theoretical density was lower than the measured. This phenomenon may be caused by the little bit higher infiltration pressure required because of the bad wetting between the Al99.5 and the microspheres. In the case of the AlSi12 matrix (when the infiltration pressure was lower due to somewhat better wetting); the unintended porosity had a positive value, which means, the pressure was not enough to force the matrix material among the small microspheres and therefore the unintended porosity became higher and the density became lower. From this, it can be deduced that lower density would be advantageous but not by the lack of matrix material. The unintended porosities are formed between the microspheres especially where three microspheres are connected.

After the density and porosity calculations and measurements, the X-ray investigations were completed. Table 4 shows the phase constitution of pure aluminium matrix syntactic foams. According to the results, which were obtained by evaluation of X-ray diffractograms, the Al-SL300 type MMSF has a significantly different phase composition than the others. Table 5 presents phase

Table 3 Calculated and measured density and porosity values of the MMSFs

Specimen	Density		Average radius		Porosity		
	Theoretical (gcm^{-3})	Measured (gcm^{-3})	Outer (μm)	Inner (μm)	Planned (−)	Unintended (−)	Total (−)
Al-SL150	1.3442	1.4273	50	46.31	0.509	−0.062	0.447
Al-SLG	1.3833	1.4635	65	59.65	0.495	−0.058	0.437
Al-SL300	1.4178	1.5197	75	68.25	0.482	−0.072	0.410
AlSi-SL150	1.3226	1.3076	50	46.31	0.509	0.011	0.520
AlSi-SLG	1.3617	1.3340	65	59.65	0.495	0.020	0.515
AlSi-SL300	1.3962	1.3698	72	68.25	0.482	0.019	0.501

Orbulov and Dobranszky [22]

Table 4 Phase constitution of Al99.5 matrix syntactic foams (wt%)

Specimen	Al	Si	Mullite	γ-Al_2O_3	α-Al_2O_3	Amorphous
Al-SL150	67	8	11	11	3	0
Al-SLG	63	6	14	11	4	0
Al-SL300	78	0	11	0	0	11

Table 5 Phase constitution of AlSi12 matrix syntactic foams (wt%)

Specimen	Al	Si	Mullite	Quartz	Amorphous
AlSi-SL150	72	7	13	0	8
AlSi-SLG	72	7	13	0	8
AlSi-SL300	72	7	12	0.5–1.0	8

composition of the AlSi12 matrix syntactic foams; notably, there is no difference between the samples.

Due to an exchange reaction, SiO_2 was reduced by the Al in syntactic foams with Al99.5, thus Al_2O_3 and elementary Si were formed according to the following equation ($\Delta G = -310$ to -313 kJ mol^{-1}, 700–850 °C) [10, 23, 24].

$$4Al_{(liq)} + 3SiO_{2(sol)} \rightarrow 2Al_2O_{3(sol)} + 3Si_{(sol)} \quad (4)$$

This diffusion type reaction strongly depends on the infiltration temperature and the exposure time. The driving force of the diffusion was the Si-concentration difference between the microsphere walls and the matrix material. As for the Al99.5 matrix, Al_2O_3 was formed according to the exchange reaction while the amorphous phase and mullite phase contents decreased significantly. Al_2O_3 was developed mainly as γ-Al_2O_3, and less α-Al_2O_3 due to diffusion process. During the Al_2O_3 formation the filler walls were degraded and elementary Si was precipitated along them as showed in Fig. 1a and b.

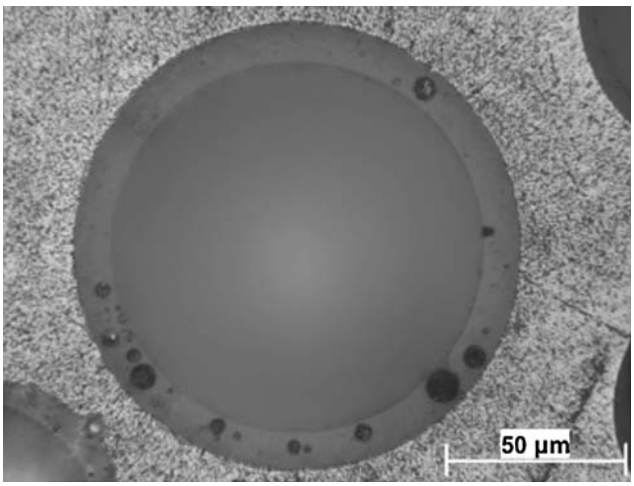

Fig. 2 Micrograph of a hollow microsphere in the Al-SL300 type syntactic foam

As one can see in Table 4, the Al-SL300 type composite can be qualified as an exception. The mullite content decreased, but no Al_2O_3 and Si were formed, and some amorphous phase remained. The hollow microspheres remained unharmed as shown in Fig. 2. This can be explained by the lower infiltration temperature (690 °C) and the somewhat smaller specific surface area (surface/volume ratio) of the SL300 type hollow microspheres. According to these results (Table 4) it is clear, that X-ray investigation on powdered samples is excellent way to make sure of the occurrence of the change reaction.

In the case of the AlSi12 matrix the mullite and Si contents were decreased too, but to a smaller degree, and there was no Al_2O_3 formation. This fact implies that the exchange reaction (refer to Eq. 4) was suppressed or blocked. As mentioned above, the driving force of the

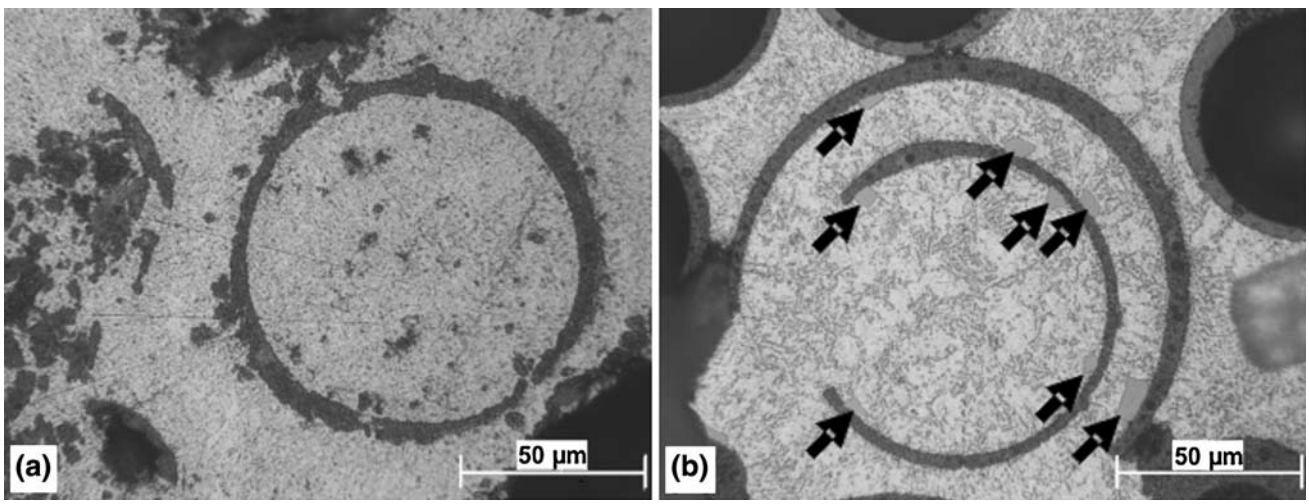

Fig. 1 Cross section of broken and degraded (**a**) microsphere walls, surrounding Si precipitations, marked by *arrows* (**b**) in the Al-SLG type syntactic foams

exchange reaction was the Si concentration difference between the hollow microsphere walls and the matrix material. This was decreased in the case of the AlSi12 matrix, which contains a considerable amount of Si. Due to this, the driving force decreased and the rate of the exchange reaction decreased, too. Because of the suppressed reaction, the microsphere walls remained unharmed and well defined as shown in Fig. 3a and b. However, the quartz content of the AlSi-SL150 and the AlSi-SLG type foams were transformed. It was unchanged in the AlSi-SL300 type foam because of the reduced infiltration temperature (600 °C) and lower specific surface.

The eutectic matrix material and the unharmed hollow microspheres can be clearly seen in Fig. 3. Some small elementary Si precipitations can also be observed. These precipitations originated from the AlSi12 matrix.

Considering the possibility of chemical reactions between the microspheres and the matrix materials, it is worth mentioning that, the ceramic microspheres can be used as a source of alloying elements in MMSF systems. The appropriate choice and concentration of alloying element in the wall material or in a surface coating [17] of the microspheres can result in precipitation, grain refinement, and microstructure as per the designed scheme. These alloying elements can enhance the mechanical and/or other properties of the MMSFs. However, there is an effective range of the alloying due to the limited time after infiltration to cooling. If the effective distance between the microspheres is small enough, it is possible to guarantee a homogenous microstructure. If the distance is larger, then the alloying effects are only in the vicinity of the microspheres.

EDS line measurements were performed on polished specimens. The line-scan profiles showed the alternating of chemical elements along the line. This offers a very good opportunity to examine the interface layer and the changes in the hollow microsphere wall in the matrix. Examples for the Al99.5 and the AlSi12 matrices are shown in Figs. 4 and 5, respectively. In Fig. 4, the wall of an SL150 type hollow microsphere can be observed in high magnification back-scattered electron (BSE) image.

It can be seen that the outer edge of the wall is not very well defined. This means that the surface of the microsphere is degraded. As mentioned above, the exchange reaction produces Al_2O_3, which is advantageous, but not at a price of degrading the hollow microsphere's wall. The diffusion process made a relatively wide interface layer on the outer surface of the hollow microspheres (i.e. from point B to point C). The width of the interface layer was ($\sim$6 μm) and it was measured between the significant changes of the derivation of the curves showing the changing of the Al. Along the interface the Si and Al contents increased and decreased, respectively, with a moderate slope. After point C the Al, O and Si contents were constants according to the actual composition of the wall. From point D the measurement is not reliable because of the curvature of the inner surface of the hollow microsphere.

In the case of the AlSi12 matrix the Al and Si content can be clearly observed at the beginning of the diagram.

The outer surface was unharmed as the exchange reaction was suppressed. Points B and C were very close to each other. This indicates that there is a very narrow (i.e. less than 3 μm) observable interface layer. The sharp, but not totally vertical transition between points B and C, is as a result of excitation conditions of the electron beam microanalysis. The lack of interface layer on the outer surface indicates that the change reaction was suppressed in these high silicon-containing MMSFs. In the concentration-sensitive BSE image, lighter needle-like phases can be observed in the wall of SL150 spheres.

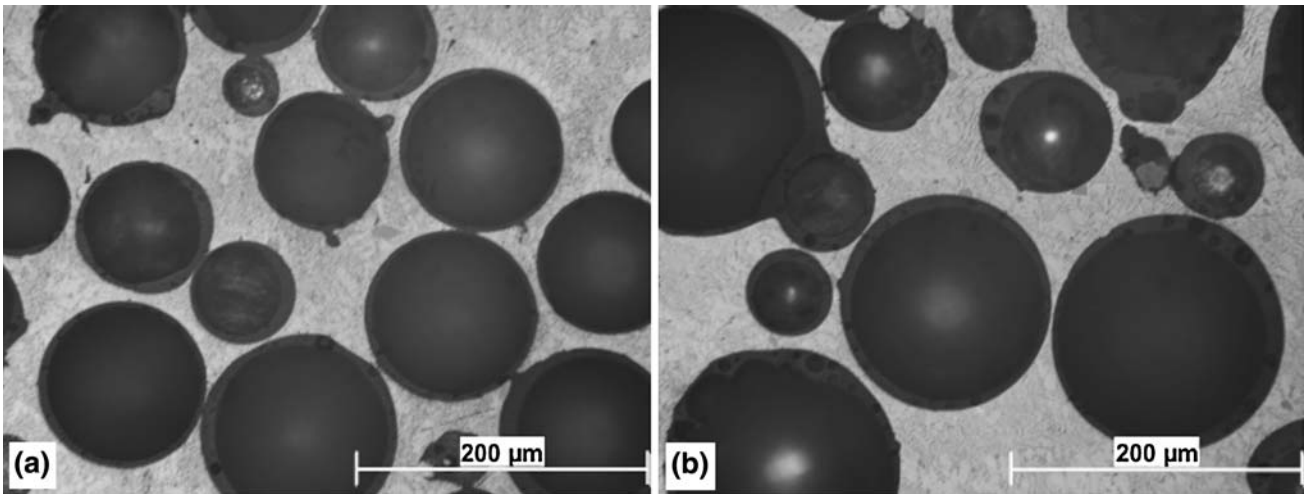

Fig. 3 Micrograph of the AlSi12-SL150 (**a**) and the AlSi12-SLG (**b**) type syntactic foams

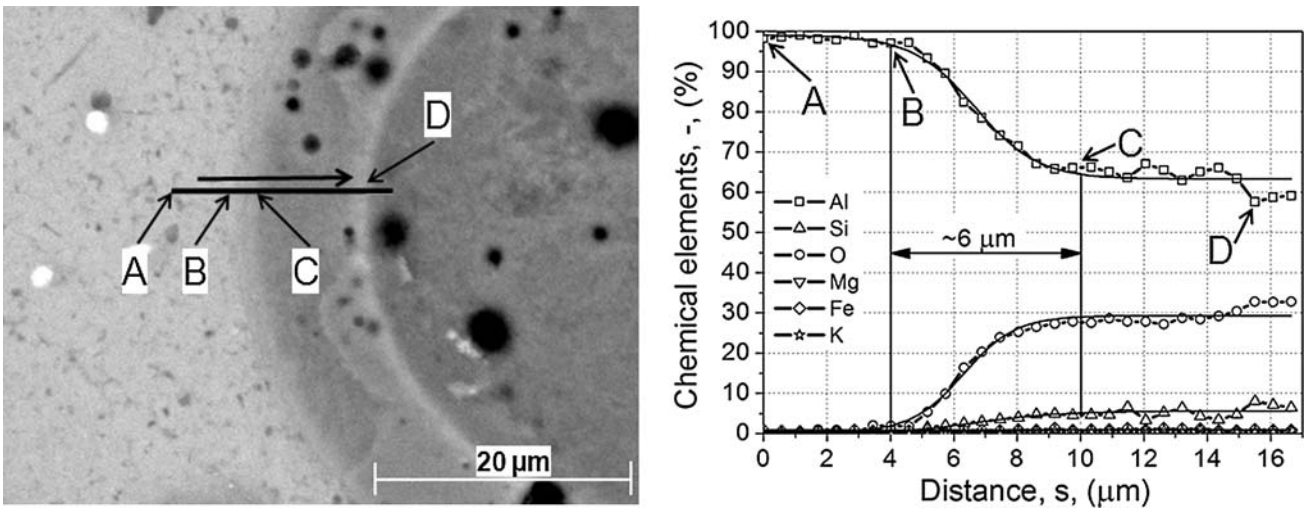

Fig. 4 BSE image and EDS line-scan profiles (with *fitted curves*) of the Al-SL150 syntactic foams

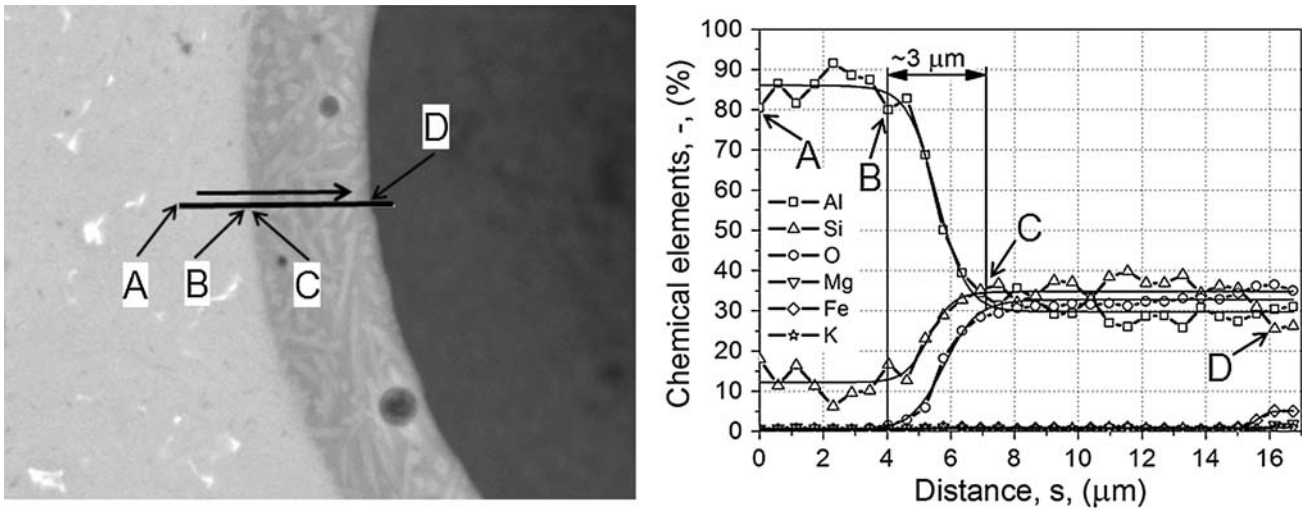

Fig. 5 BSE image and EDS line-scan profiles of the AlSi12-SL150 syntactic foams

According to this a well-defined Al and Si, alternation occurred in the line of EDS analysis diagram. In the lighter areas, the Si content decreased while the Al content increased. The oxygen content remained constant. This implies that lighter phases in the wall of hollow microspheres are Al_2O_3 rich particles (mullite) embedded in SiO_2 rich matrix. At point D, on the inner side of the hollow microsphere wall, a very narrow Fe, Mg and K rich zone can be observed (originated from the various oxides of the hollow microspheres).

Conclusions

Ceramic hollow microsphere filled aluminium matrix metallic foams were produced, and the possible reactions which can be taken place in the interfaces, were investigated by determining the phase and elemental composition of the MMSFs. From the results of the XRD and the EDS measurements described above, the following statements can be made.

In the Al99.5 matrix syntactic foams intensive α- and γ-Al_2O_3 formation occurred due to an exchange reaction, except in the case of the SL300 type reinforcement. These alumina phases formed in the reductive reaction of the amorphous SiO_2 by the molten aluminium. The driving force of this diffusion controlled reaction was the Si concentration gradient between the microspheres and the matrix. The interface was damaged and cannot be so easily separated. The reaction between the microsphere and the matrix degraded the hollow microspheres' wall. The infiltration temperature has a strong influence on the kinetics of

the change reaction. That is why there was no reaction in the case of the Al-SL300 type syntactic foams infiltrated at lower (690 °C) temperature. This indicates that there is a limit relating to the temperature. Above this temperature the change reaction is intensive, but below the temperature limit, the reaction will not occur. The specific surface area (surface/volume ratio) of the hollow microspheres also affected the kinetics of the change reaction. These parameters are extremely important for successful and effective syntactic foam production.

As for the AlSi12 matrix syntactic foams, the exchange reaction were suppressed by the considerable amount of the Si in the matrix alloy: there were no interface layers between the hollow microspheres and the matrix. The wall of the hollow microspheres remained unharmed. This means, that when silicon content of the matrix is near to the solubility limit, the ceramic hollow microspheres can preserve their structural integrity. Therefore, the AlSi12 matrix syntactic foams seem to be a much better choice for structural applications. In the case of the AlSi-SL300 syntactic foam the quartz content was not transformed due to reduced infiltration temperature (600 °C).

In general, X-ray investigations on powdered samples are an excellent way to ensure the occurrence of any change reactions.

The ceramic microspheres can be used as a source of alloying elements in MMSF systems. The appropriate choice and concentration of alloying element in the wall material or in a surface coating of the microspheres can enhance the properties of the MMSFs. The alloying is a diffusion characterised process and it has an effective range because the limited reaction time and temperature. These process parameters can be changed, if necessary, to provide better alloying and better mechanical properties.

Acknowledgements Special thanks to Professor J.T. Blucher for his kind support and to I. Sajo for XRD measurements. The Metal Matrix Composites Laboratory is supported by Grant # GVOP 3.2.1-2004-04-0145/3.0. The investigations were supported by The Hungarian Research Fund, NKTH-OTKA K69122. Thanks to R. Toth and C. H. Erbsloh Hungaria Speciality and Industrial Minerals Ltd. for providing E-spheres.

References

1. Kallas DH, Chatten CK (1969) Ocean Eng 4:421
2. Gupta N, Kishore, Woldesenbet E, Sankaran S (2001) J Mater Sci 36:4485. doi:10.1023/A:1017986820603
3. Gupta N, Woldesenbet E, Kishore (2002) J Mater Sci 37:3199. doi:10.1023/A:1016166529841
4. Woldesenbet E, Gupta N, Jadhav A (2005) J Mater Sci 40:4009. doi:10.1007/s10853-005-1910-2
5. Fine T, Sautereau H, Sauvan-Moynot V (2003) J Mater Sci 38:2709. doi:10.1023/A:1024403123013
6. Islam MM, Kim HS (2007) J Mater Sci 42:6123. doi:10.1007/s10853-006-1091-7
7. Ramachandra M, Radhakrishna K (2005) J Mater Sci 40:5989. doi:10.1007/s10853-005-1303-6
8. Ramachandra M, Radhakrishna K (2007) Wear 262:1450
9. Rohatgi PK, Guo RQ, Iksan H, Borchelt EJ, Asthana R (1998) Mater Sci Technol A 244:22
10. Rohatgi PK, Kim JK, Gupta N, Alaraj S, Daoud A (2006) Compos Part A 37:2006
11. Balch DK, O'Dwyer JG, Davis GR, Cady CM, Gray GTIII, Dunand DC (2005) Mater Sci Eng A 391:408
12. Rajput V, Mondal DP, Das S, Ramakrishnan N, Jha AK (2007) J Mater Sci 42:7408. doi:10.1007/s10853-007-1837-x
13. Dou ZY, Jiang LT, Wu GH, Zhang Q, Xiu ZY, Chen GQ (2007) Scripta Mater 57:945
14. Wu GH, Dou ZY, Sun DL, Jiang LT, Ding BS, He BF (2007) Scripta Mater 56:221
15. Kiser M, He MY, Zok FW (1999) Acta Mater 47:2685
16. Zhang LP, Zhao YY (2007) J Compos Mater 41:2105
17. Palmer RA, Gao K, Doan TM, Green L, Cavallaro G (2007) Mater Sci Eng A 464:85
18. Bárczy T, Kaptay Gy (2005) Mater Sci Forum 473–474:297
19. Trumble PK (1998) Acta Mater 46:2363
20. Balch DK, Dunand DC (2006) Acta Mater 54:1501
21. Envirospheres Pty. Ltd. http://envirospheres.com
22. Orbulov IN, Dobranszky J (2008) Period Polytech Mech Eng 52
23. Weast RC (1990) CRC handbook of chemistry and physics, 70th edn. CRC Press, Boca Raton, FL, p D-33
24. Samsonov GV (1973) The oxide handbook. IFI/Plenum Data Corporation, New York, p 122